Broadband heterogeneous terahertz frequency quantum cascade laser

L. H. Li, K. Garrasi, I. Kundu, Y. J. Han, M. Salih, M. S. Vitiello, A. G. Davies, and E. H. Linfield

We demonstrate a broadband, heterogeneous terahertz frequency quantum cascade laser by exploiting an active region design based on longitudinal optical (LO)-phonon-assisted interminiband transitions. We obtain continuous wave laser emission with a threshold current density of ~120 A/cm^2, a dynamic range of ~3.1, and an emission spectrum spanning from 2.4 to 3.4 THz at 15 K.

Introduction: Terahertz (THz) frequency quantum cascade lasers (QCLs) are compact and powerful solid-state semiconductor sources that deliver up to Watt-level pulses of radiation in the 1.2 – 5.6 THz range [1]. Furthermore, they can be engineered to have a very broad gain bandwidth, enabling the spontaneous formation of THz frequency combs [2-5], which have very significant applications in high resolution and high precision spectroscopy [6, 7].

To achieve broadband frequency combs using a QCL, one of the most promising approaches is to stack different quantum cascade active regions (ARs), with individually designed emission frequencies, into the same laser waveguide [8]. Using this approach at THz frequencies, and utilising the strong optical field confinement of a double-metal (DM) waveguide, octave-spanning THz QCLs were recently demonstrated using ARs based on a four-quantum well, bound-to-continuum design that exploited longitudinal optical (LO) phonon extraction [2, 3]. However, broadband operation from such THz QCLs was generally observed over only a very small current density dynamic range, $JDR = J_{max}/J_{th}$ [2, 3], where J_{th} is the threshold current density and J_{max} is the maximum working current density. This arose from the differences of J_{th} and J_{max} between the individual ARs, which meant that the full broadband spectrum was only observed when the injection current density in the heterogeneous laser cavity was significantly higher than J_{th} for each individual AR [4]. The effective working current range of the whole heterogeneous THz QCL was thus very small. One possible approach to increase the JDR of a broadband THz QCL is to increase the AR doping density (n_d). Unfortunately, this also leads to an increased J_{th}, and an increased dissipated electrical power, which causes a significant deterioration in the continuous wave (CW) performance [3]. To avoid this, alternative AR designs with lower J_{th} and larger JDR are highly desirable. Recently, an AR design consisting of nine GaAs quantum wells, forming a cascade of alternating photon and LO-phonon-assisted transitions between two quasi-minibands has been developed [9]. It has proved to have a low J_{th}, large JDR, high CW working temperature, and to yield high output powers at low applied biases [9, 10]. In this letter, we develop broadband heterogeneous THz QCLs with low J_{th} and large JDR by exploiting this type of AR design.

Experimental details: To obtain a QCL with a 1 THz bandwidth, the design from ref. [9] was rescaled to form several individual ARs, each operating at a different frequency; these were then stacked together and embedded into a double metal waveguide. The number of periods, the order of the ARs, and n_d were carefully arranged to give a flat gain and uniform power output across the whole spectrum.

Two types of structures were grown by solid-source molecular beam epitaxy on semi-insulating GaAs substrates: homogeneous stacks in which the rescaled ARs were grown individually, and the heterogeneous design. The complete structures consist of a 250 nm undoped GaAs buffer layer, an undoped 300 nm Al$_{0.5}$Ga$_{0.5}$As etch-stop layer, an Si-doped (2x10^{18} cm^{-3}) GaAs layer (700 nm thick for a single-plasmon waveguide, or 70 nm thick for DM waveguides), the AR, and a 50 nm heavily Si-doped (5x10^{18} cm^{-3}) GaAs top contact layer. After growth, the homogeneous QCL wafers were processed into single-plasmon waveguide structures to enable the designs to be optimized, whilst the heterogeneous QCL wafers were processed into a DM waveguide structure with side absorbers for broadband emission [2, 3].

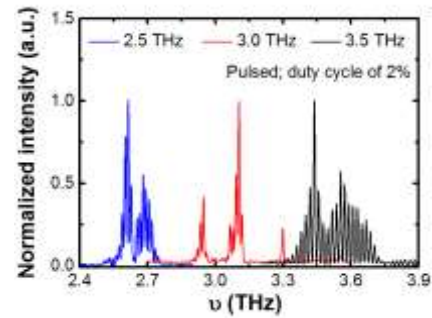Devices were cleaved and indium-soldered onto copper submounts for measurement.

Fig. 1 *Typical lasing spectra measured in pulsed mode at 10 K for three homogeneous QCLs, of different AR designs, targeted at frequencies of 2.5, 3.0 and 3.5 THz.*
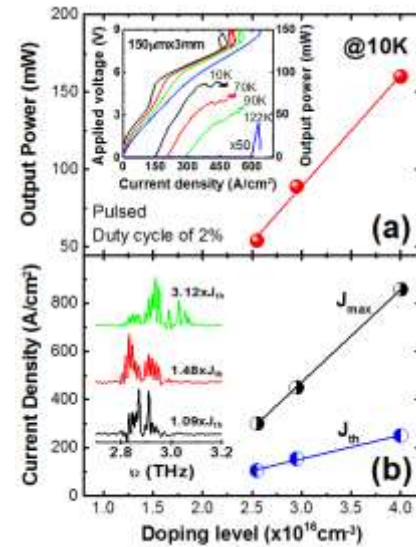

Fig. 2 *(a) P_{peak}, and (b) J_{th} and J_{max}, of 3 THz QCLs as a function of n_d at 10 K. Inset (a): Typical LIV characteristics of an as-cleaved 3 THz QCL as a function of the heat sink temperature. Inset (b): Typical emission spectra of the device as a function of injection current density.*

Results: Fig. 1 shows the typical lasing spectra at 10 K from three homogeneous QCLs, of different AR designs, targeted at frequencies of 2.5, 3.0 and 3.5 THz. The devices were measured in pulsed mode (duty cycle of 2 %). Similar to ref. [9], the layer sequences of these AR designs are respectively 10.6/**0.5**/17/**1**/13.5/**2.1**/12.4/**3.1**/10/**3.1**/9/**2.9**/7.5/**3.1**/<u>17.8</u>/**3.1**/15.2/**4.1**, 9.8/**0.5**/15.7/**1**/12.5/**2**/11.4/**2.9**/9.2/**2.9**/8.3/**2.9**/6.9/**2.9**/<u>16.5</u>/**2.9**/14.1/**3.9**, and 10.5/**0.5**/12.2/**1**/12.5/**1.9**/11/**2.8**/8.8/**2.8**/7.9/**2.8**/6.6/**2.8**/ <u>15.8</u>/**2.8**/13.8/**3.7**, where the thickness is in nanometres, the bold figures represent the AlGaAs barriers, and the underlined figures denote the Si-doped GaAs layer. The aluminium content in the barriers of these AR designs is 0.14, 0.16 and 0.18, respectively. Since two optical transitions are involved in the lasing process, the lasing spectrum is inherently broad up to about 0.4 THz for each AR design, consistent with the observations in ref. [9]. This broad spectrum makes it very attractive to stack these ARs together into the same waveguide to obtain a broadband frequency comb.

Fig. 2 shows the peak output power (P_{peak}), J_{th} and J_{max} of a set of 3 THz QCLs as function of n_d at 10 K. The data were acquired in pulsed mode from devices fabricated from the homogeneous wafers with a nominally identical AR design but different n_d. For comparison, all devices had similar dimensions of 150 μm x 3 mm. It is observed that P_{peak}, J_{th} and J_{max} are proportional to n_d, as expected [11, 12]. Specifically, as n_d increases from 2.6 x 10^{16} cm^{-3} to 4.0 x 10^{16} cm^{-3}, P_{peak}, J_{th} and J_{max} increase from 55 mW to 160 mW, 106 A/cm^2 to 250 A/cm^2, and 300 A/cm^2 to 857 A/cm^2, respectively. It is interesting to note that J_{th} is less sensitive to n_d than J_{max}, and so JDR increases from 2.85 to 3.43 as n_d increases. Typical output power-current-voltage

(LIV) characteristics of an as-cleaved device (n_d =3x10^{16}cm^{-3}) are presented as a function of heat sink temperature in the inset of Fig 2 (a). The device operates up to 122 K in pulsed operation and 65 K in CW (data not shown). Typical emission spectra of the 3 THz QCLs are plotted as a function of current density in the inset of Fig 2 (b). With increasing injection current density, a broader spectrum is observed.

Table 1: Summary of the performance at 10 K of typical (~ 3mm x 150 µm) devices fabricated from the homogeneous wafers with three different AR designs.

Design		n_d (cm^{-3})	J_{th} (A/cm^2)	J_{max} (A/cm^2)	P_{max} (mW)	T_{max} (K)	ν (THz)
2.5 THz	W1	3.0x10^{16}	195	470	55	113	2.5-2.75
	W2	3.2x10^{16}	200	480	75	112	2.54-2.85
3.0 THz	W3	2.6x10^{16}	106	300	55	107	2.85-3.3
	W4	3.0x10^{16}	154	500	89	121	2.8-3.2
3.5 THz	W5	2.6x10^{16}	125	400	45	127	3.3-3.7
	W6	3.0x10^{16}	140	470	85	115	3.25-3.6

Table. 1 summarizes the performances at 10 K of typical devices fabricated from six wafers (W1 – W6) with the homologous design. The device performances are very similar at the three frequencies, with the slight differences between wafers with the same AR design being attributed to slightly different n_d. All devices show $J_{th} \leq 200$ A/cm^2 and P_{peak} of several tens of mW, suggesting the suitability of these wafers for use in fabricating high power CW devices. The largest JDR of 3.36 was obtained from the 3.5 THz design, whilst the smallest JDR of 2.41 was found in the 2.5 THz design. These values are much larger than the best value of ~2 reported in ref. [11] where THz QCLs based on the four-quantum well design were used, and where furthermore JDR falls as n_d increases. As a result of the large JDR, these ARs ought to enable a large dynamic range when stacked together to form a broadband AR. A heterogeneous wafer with n_d of 3 x 10^{16} cm^{-3} was therefore grown in the sequence: 40 periods of the 3.5 THz design, 40 periods of the 3.0 THz design, and 55 periods of the 2.5 THz design.
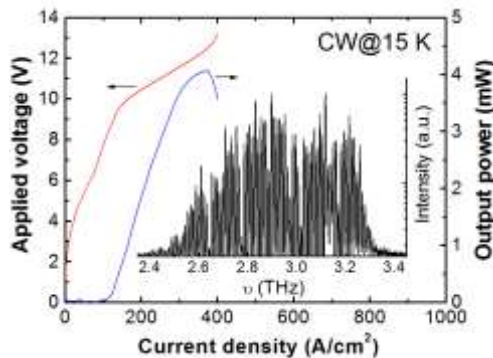

Fig. 3 *Typical CW LIV characteristics at 15 K of a 60 µm x 2.9 mm DM waveguide heterogeneous THz QCL with 2 µm absorbers on both sides of the device ridge. Inset: emission spectrum of the device at 2.1 x J_{th}.*

Fig. 3 shows typical CW LIV characteristics at 15 K of a 60 µm x 2.9 mm, DM waveguide, heterogeneous THz QCL with 2 µm absorbers on both sides of the device ridge [2, 3], with the inset showing the emission spectrum of the device at 2.1 x J_{th}. The device has a J_{th} of ~120 A/cm^2, a JDR of ~3.1, P_{peak} up to ~4 mW, and a spectrum spanning from 2.4 to 3.4 THz. In addition, CW operation was observed up to 72 K. Compared to the octave-spanning THz QCLs demonstrated in ref. [2], the device in the present work has J_{th} reduced by a factor of ~2, the JDR almost doubled, and the maximum CW working temperature increased by ~17 K. This demonstrates that an LO-phonon-assisted interminiband transition AR design is very promising for the design of broadband THz QCLs, whilst further optimisation is expected to lead to an even broader frequency span. It should be noted that frequency combs have already been observed from this wafer, and verified by beat-note measurements [13], which will be presented elsewhere.

Conclusion: We have developed heterogeneous broadband THz QCLs by exploiting an LO-phonon-assisted interminiband transition AR design. The device operated in CW mode with a J_{th} = 120 A/cm^2, a JDR = 3.1, and showed an emission spectrum spanning 1 THz bandwidth (2.4 – 3.4 THz) at 15 K.

27 *June 2018*

L. H. Li, I. Kundu, Y. J. Han, M. Salih, A. G. Davies, and E. H. Linfield (*School of Electronic and Electrical Engineering, University of Leeds, Leeds LS2 9JT, United Kingdom*)

Katia Garrasi and M. S. Vitiello (*NEST, CNR—Istituto Nanoscienze and Scuola Normale Superiore, Piazza San Silvestro 12, 56127, Pisa, Italy*)

E-mail: l.h.li@leeds.ac.uk

References

[1] LI, L. H., et al.: 'Terahertz quantum cascade lasers with >1 W output powers', *Electron. Lett.* 2014, **50** (4), pp.309.

[2] RÖSCH, M., et al.: 'Octave-spanning semiconductor laser', *Nat. Photonics*, 2015, **9**, pp.42.

[3] RÖSCH, M., et al.: 'Heterogeneous terahertz quantum cascade lasers exceeding 1.9 THz spectral bandwidth and featuring dual comb operation', *Nanophotonics,* 2018, **7**, pp.237–242.

[4] TURČINKOVĂ, D., et al.: 'Ultra-broadband heterogeneous quantum cascade laser emitting from 2.2 to 3.2 THz', *Appl. Phys. Lett.* 2011, **99**, pp. 191104.

[5] BURGHOFF, D., et al.: 'Terahertz laser frequency combs', *Nat. Photonics,* 2014, **8**, pp.462–467.

[6] FAIST, J., et al.: 'Quantum Cascade Laser Frequency Combs', *Nanophotonics* 2016, **5**, pp. 272–291.

[7] BARTALINI, S., et al.: 'Frequency-Comb-Assisted Terahertz Quantum Cascade Laser Spectroscopy', *Phys. Rev. X,* 2014, **4**, pp.021006.

[8] GMACHL, C., et al.: 'Ultrabroadband semiconductor laser', *Nature*, 2002, **415**, pp. 883.

[9] WIENOLD, M., et al.: 'Low-voltage terahertz quantum cascade lasers based on LO-phonon-assisted interminiband transitions', *Electron. Lett.* 2009, **45** (20), pp.1030-1031.

[10] WIENOLD, M., et al.: 'High-temperature, continuous-wave operation of terahertz quantum-cascade lasers with metal-metal waveguides and third-order distributed feedback', *Opt. Express,* 2014, **22**, pp. 3334-3348.

[11] AMANTI, M. I., et al.: 'Bound-to-continuum terahertz quantum cascade laser with a single-quantum-well phonon extraction/injection stage', *New J. Phys.*, 2009, **11**, pp.125022.

[12] LI, L. H., et al.: 'The MBE growth and optimization of high performance terahertz frequency quantum cascade lasers', *Opt. Express,* 2015, **23** (3), pp. 2720.

[13] VITIELLO, M. S., private communication.